

## Chapter 3

# Molecular Dynamics Method

In the present Chapter we consider the first among the two main methods of modeling used in physics, the Molecular Dynamics (MD) method. It consists in computer modeling of motion of a “sufficiently large” number of particles with a given interaction law. The word “molecular” in the name of the MD method has a historical origin; in a real system electrons, atoms, molecules, quasiparticles (e.g., solitons), planets, stars, galaxies, *etc.* may play the role of “molecules” as well. The motion of particles is usually assumed to be classical, i.e. they move according to Newton’s laws. For an atomic systems, an effective interaction potential which approximately takes into account quantum corrections to the interaction law, may be used [69].

The MD method is used for investigation of systems which either have no analytical description at all, or have an analytical description but its accuracy and the region of its validity are unknown. In the latter case, the results of MD modeling are used as an “etalon”, i.e., as the “obtained from the first principles exact solution” which could then be compared with the results of different approximate approaches. First of all we have to mention the systems which are far from the thermal equilibrium state. Investigation of dynamical characteristics of the thermodynamically equilibrium state by the MD modeling leads to important and interesting results too. Last, investigation of thermodynamical characteristics such as properties of phase transitions by the MD method is useful too, although in the latter case the Monte Carlo method is more suitable usually.

As has been mentioned in Introduction, computer modeling in many points looks like a laboratory experiment and, moreover, it has a series of important advantages. First, in the computer experiment we can make a snapshot and analyze the positions of all particles in the system at any given time moment. Often it is useful also to plot the trajectories of particles during some time interval. Clearly that to obtain such pictures in laboratory experiments is impossible in principle. Second, with the help of computer modeling we can investigate the system behavior under the conditions which cannot be achieved in a real experiment. For example, we may heat up a plasma to as high temperature as we want, artificially restricting the system volume using appropriate boundary conditions. Third, in the computer experiment we can investigate the systems which are inaccessible for us in a laboratory. For example, we can study star collisions, evolution of galaxies, *etc.*

As an illustration, let us describe an example where a single star collides with a double star [70]. Figure 3.1 shows star trajectories for one particular choice of initial conditions. As seen, the process is rather complicated. Depending on initial conditions (such as the target parameter, i.e. the shortest distance between the single star and the center of the double system, and the orbital phase, i.e. the relative positions of stars in the double star in the initial configuration), one of the following three scenarios may take place: **(a)** the “fly past”, when the orbital phase of the double star has been changed in the collision process, but the double star remains to exist as a whole (Fig. 3.2a), **(b)** the “exchange”, when the single star replaces a star in the double system (Fig. 3.2b), and **(c)** the “ionization”, when all three stars occur to become uncoupled in the final state (Fig. 3.2c). The results of modeling of more than  $10^3$  experiments are summarized in the diagram in Fig. 3.3.

In the example described above the MD method has been used to model the motion of three particles.

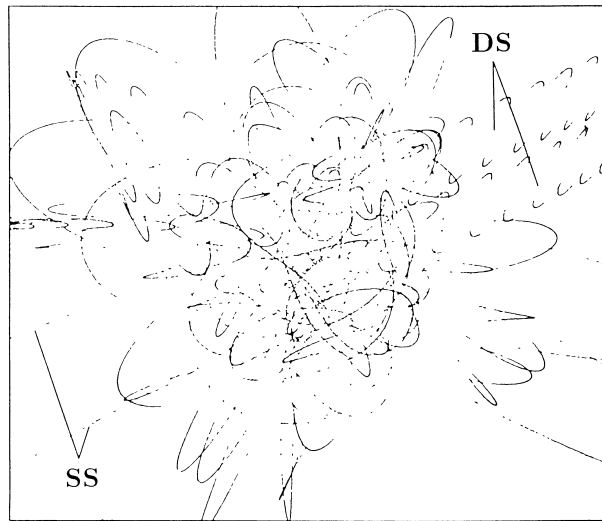


Figure 3.1: Trajectories of stars' motion for one particular choice of initial conditions as calculated in [70]. **SS** indicates the trajectory of the single star, and **DS**, that of the double system.

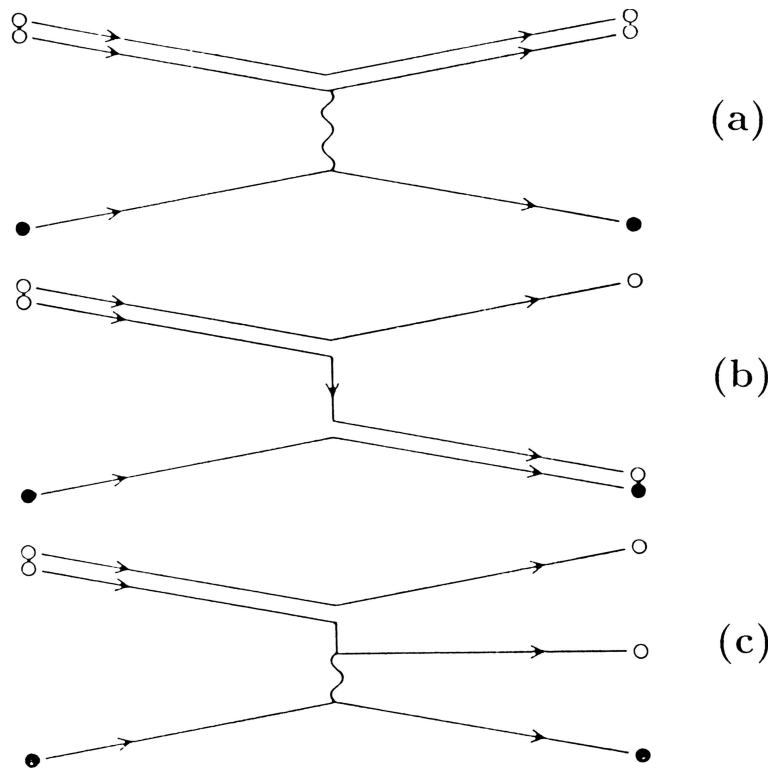


Figure 3.2: Schematic presentation of different stars' collision scenarios: (a) fly past, (b) exchange, and (c) ionization (from [70]).

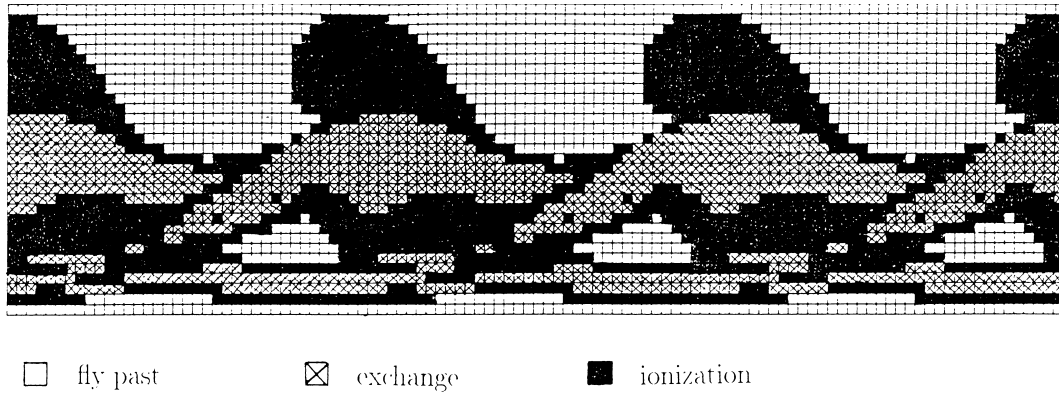


Figure 3.3: Diagram for different events at stars' collision for different initial conditions as calculated in [70].

Sometimes, as, for example, in the Henon-Heiles model (Sec. 2.1), the MD method is used to study the motion of a single particle only. In modeling of physical systems, however, a more typical is the situation when the number of particles should be as large as possible, and this number is restricted by the computer power only. In fact, the number of particles in the MD method is about  $10^2 \div 10^3$ , and up to  $10^6$  in the extreme cases. An answer on the question, is this number sufficient for that the physical situation being described correctly, first of all depends on the dimensionality of the model under consideration. For example, in modeling of one-dimensional systems, a chain of  $10^3$  atoms is practically undistinguishable from the infinite chain. But when we study three-dimensional systems, a cube of  $10^3$  atoms has the linear extension of 10 atoms, so in the latter case the model describes properties of a small cluster rather than the bulk properties of a solid state.

The MD modeling was, is, and (at least in a near future) will be a sufficiently expensive job. Usually we can make a small number of computer experiments only, and we may vary a restricted number of model parameters. Thus, the model under consideration as well as the method of its solution should be chosen with a special care. Below in Sections 3.2 to 3.4 we consider several characteristic examples of MD modeling. First, however, let us present some general principles which would be used in choosing of models and methods for their solution.

### 3.1 General statements

First of all we have to settle the model dimensionality. There exist one-dimensional (1D) models where atoms move along one coordinate only, two-dimensional (2D) models where atoms are aligned with a plane, and three-dimensional (3D) models. Sometimes, one- or two-dimensional models for a system of atoms inserted into an external (usually periodic) potential are used. For example, in the two-dimensional system of atoms adsorbed on a crystal surface, the substrate periodic potential plays the role of the external potential.

Of course, real physical objects are placed into three-dimensional space always. On the other hand, except some specific problems, linear extension of the system should be sufficiently large. Therefore, if it is possible, the priority should be given to one- or two-dimensional models. But such a possibility may not exist at all. The most striking examples of situations where the one-dimensional model incorrectly describes the physical situation, are the problem of validity of statistical physics laws (where the use of the 1D model leads to the Fermi-Pasta-Ulam paradox, see below Sec. 6.1), and the problem of phase transitions (one-dimensional systems do not exhibit phase transitions at all for any  $T > 0$ ).

Because in numerical experiments the number of particles is finite always, the question on boundary conditions arises. The following three types of boundary conditions are used typically:

(a) *Free boundary conditions.* In this case there are no additional conditions for the boundary atoms of the model's volume. Note, however, that the atoms at the boundary are in special conditions because they

have neighbors from one-hand side only. Of course, the free boundary conditions can only be used when the atoms attract each other at large distances at least, because otherwise the atoms will run away from the system in opposite directions.

(b) *The fixed boundary conditions*, when the coordinates of the boundary atoms are fixed and their velocities are artificially put to zero, i.e. the boundary atoms are excluded from the MD modeling. Sometimes the following modification of this method is used (the so-called “damped boundary conditions”): additionally to pinning of the boundary atoms, some conditions are imposed on few “marked” atoms (or atomic layers) located near the boundaries. For example, while the motion of atoms in the system is subjected to Newton’s laws, the motion of the “marked” atoms is described by the motion equations with a viscous friction, and the value of the friction coefficient smoothly increases with approaching to the boundary (from zero for “bulk” atoms to infinity for boundary atoms). In this case impulses or waves which go to the boundary region, are damped in this region and cannot go back to the bulk of the system. In the result, dynamical properties of such system will remind those of the infinite system where also a wave going to infinity, cannot be returned back. An another example of modified boundary conditions is the case when motion of atoms near the boundary is described by the Langevin equations (see below Chapter 4); in this case we can model a system in contact with a thermostat at a nonzero temperature.

It is important to note that in the cases of the free or fixed boundary conditions, we must exclude the boundary and “marked” atoms from the consideration if we are interesting in “bulk” system properties.

(c) May be, the most popular are the *periodic*, or *cyclic (Born-Karpman) boundary conditions*. For example, if we study a one-dimensional model, then in order to impose the periodic boundary conditions on the chain of  $N$  atoms, we have to introduce a fictitious  $(N + 1)$ -th atom which is assumed to move analogously to the first atom in the chain. In other words, the chain is coupled into the cycle. Similarly, one gets a tori for the two-dimensional model, and the three-dimensional tori in the case of the three-dimensional model. If the atomic system is placed into a box with a fixed volume, we have to assume that when an atom crosses the boundary and leaves the box, at the same time a new atom with the same velocity is to appear on the opposite boundary of the box. The periodic boundary conditions look to be the most attracting ones, because in this case all the atoms are treated on equal foot, and all atoms may be used for calculation of “bulk” properties. However, the cyclic conditions have their own inconveniences. Namely, imposing artificially the periodicity on the system, at the same time we introduce the minimum wave vector  $k_{\min} = 2\pi/L$  and the minimum frequency  $\omega_{\min} = 2\pi/t_{\max}$ , where  $t_{\max} = L/v_{\text{sound}}$ ,  $L$  is the linear system size and  $v_{\text{sound}}$  is the maximum sound velocity in the system. In the result the spacial Fourier spectrum of the system becomes discrete (the total momentum may take only the values which are multiplies of  $k_{\min}$ ), and the modeling is correct for times  $t < t_{\max}$  only.

When the fixed or periodic boundary conditions are used, we also have to choose a geometry for the “box” surrounding the system. In modeling of gas or liquid, the most useful way is to take the simplest box shape, i.e. to use the square (cube) box. But when we model the system which may have a crystalline structure, the shape of the box must be matched with the symmetry of this structure. Namely, the crystal must be imposed into the box without distortions, because otherwise we will artificially introduce topological defects which can not be removed during simulation.

The next important stage of model construction is a choice of the interatomic potential. In the MD modeling it is usually assumed that the interaction is pairwise and isotropic, i.e. that the potential energy of the system can be presented in the form

$$V = \sum_{i < j} v(r_{ij}), \quad (3.1)$$

where  $r_{ij}$  is the distance between the atoms with the numbers  $i$  and  $j$ . Of course, sometimes this assumption does not correspond to reality. For example, two hydrogen atoms attract one another and form the hydrogen molecule, but the coupling of a third hydrogen atom to the molecule is energetically unfavorable.

Typically one of the following functions is used for  $v(r)$ :

(a) The “hard-core” potential has the form

$$v(r) = \begin{cases} \infty & \text{if } r < a_0, \\ 0 & \text{if } r > a_0, \end{cases} \quad (3.2)$$

where  $a_0$  corresponds to the diameter of particles. Also one may use the hard-core potential with an attraction,

$$v(r) = \begin{cases} \infty & \text{if } r < a_0, \\ -v_0 & \text{if } a_0 < r < a_1, \\ 0 & \text{if } r > a_1, \end{cases} \quad (3.3)$$

where  $v_0$  is the well depth. The potentials (3.2) and (3.3) are the simplest used in the MD simulation.

(b) The power potential is described by an expression

$$v(r) = v_0 \left( \frac{a_0}{r} \right)^\nu. \quad (3.4)$$

For  $\nu = 1$  or  $\nu = 3$  this potential corresponds to Coulomb or dipole-dipole potentials respectively. As examples of applications of the potential (3.4) we can mention the interaction between electrons and ions in the ionized plasma, or the interaction of partially ionized atoms chemically adsorbed on a metal surface [71].

(c) The widely used Mie-Lennard-Jones (LJ) potential is described by an expression

$$v(r) = \frac{v_0}{\mu - \nu} \left[ \nu \left( \frac{r_0}{r} \right)^\mu - \mu \left( \frac{r_0}{r} \right)^\nu \right]. \quad (3.5)$$

This potential has the minimum of the depth  $v(r_0) = -v_0$  at  $r = r_0$ , and the frequency of vibrations near the minimum is

$$\omega_0 = \left( \frac{\mu\nu v_0}{mr_0^2} \right)^{1/2}, \quad (3.6)$$

where  $m$  is the mass of particles. The usual combination is  $\mu = 12$  and  $\nu = 6$  which describes the interaction of inert gas atoms. The first term in the right-hand side of Eq. (3.5) describes the short-range repulsion owing to overlapping of electronic shells, while the second term corresponds to the long-range van-der-Waals attraction due to mutual polarization of the atoms.

(d) The Morse potential has the form

$$v(r) = \frac{v_0}{\mu - \nu} \left[ \nu e^{-\mu\gamma(r-r_0)} - \mu e^{-\nu\gamma(r-r_0)} \right], \quad (3.7)$$

where the parameters  $r_0$  and  $v_0$  have the same meaning as in the LJ potential, and the parameter  $\gamma$  is coupled with the vibrational frequency at the minimum by the relationship

$$\omega_0 = (\mu\nu v_0 \gamma^2 / m)^{1/2}; \quad (3.8)$$

usually  $\gamma$  is taken to be  $\gamma \sim r_0^{-1}$ . The combination  $\mu = 2$  and  $\nu = 1$  is used as a rule, while another combinations may be used as well. The Morse potential is typically used to describe chemical bonds in molecules.

(e) Last, in some cases it is necessary to use the real interaction potential for  $v(r)$ . For example, such a situation emerges in modeling of the crystalline structure of metals, because the symmetry of the lattice which corresponds to the minimum of the energy, is very sensitive to the shape of the potential  $v(r)$ . In this case the function  $v(r)$  should be calculated (by solving, e.g., the corresponding Schrödinger equation for two atoms) and tabulated before the MD simulation. Then, during the simulation, a necessary value of  $v(r)$  is being found with the help of an interpolation procedure.

The choice of the concrete potential depends, of course, on the physical problem under investigation. But for other equal conditions, the preference should be given to that function  $v(r)$  which can be calculated with a shorter computer time. From this point of view the potentials **(b)** and **(c)** have the advantage before the potential **(d)**, because the operation of taking to a power is performed much more fast and accurate than the operation of taking an exponent.

The molecular dynamics method assumes the calculation of trajectories of all model particles. As a rule, the solution of motion equations is carried out by one or another modification of the Runge-Kutta method. The main requirement is, of course, the maximum accuracy of the solution. But the increase of accuracy is not a simple task. The only method of computer solution of Newtonian differential equations is to make the discretization. For this, we have to introduce a time step  $\Delta t$  and then to solve not the original differential equations but the difference equations. Of course, numerical errors at this stage are unavoidable. To decrease the errors we may, for example, to decrease the time step  $\Delta t$ . But this can be done to a certain limit only, because for too small  $\Delta t$  the resulting computation errors will overcome all gains in the accuracy. An another way to improve the accuracy consists in using the Runge-Kutta method of a higher order. But this approach leads to a sharp increase of the computation time, because the more complicated is the Runge-Kutta scheme, the longer will be the computer time of calculation of the right-hand sides of motion equations, i.e., the more is the number of times the function  $v(r_{ij})$  for all interatomic distances  $r_{ij}$  is to be calculated. On the other hand, in the MD modeling we typically need to follow for system evolution for a sufficiently long time  $t_{\max}$ . Thus, the following contradiction appears: the more accurate we will calculate the trajectories of the system motion, the shorter will be the total time of modeling  $t_{\max}$  and, therefore, the lower will be the accuracy of calculation of the averaged over time characteristics of the system. But namely the time-averaged values are typically the main goal of the MD modeling. A resolution of this contradiction would be in a compromise: the “technical” computational parameters (e.g., the time step  $\Delta t$ ) should be chosen in such a way that to achieve the maximum accuracy in the *final* results of modeling (i.e., in the time-averaged characteristics), not be too warning on accuracy of calculation of the trajectory itself. (The final choice of these “technical” parameters is carried out usually during the “training” of the program.) Moreover, for a nonintegrable system, because of the existence of an instability, the precise calculation of the trajectory (i.e., the calculation which allows to return to the initial point when all velocities are reversed) is impossible in principle.

One of methods to control the accuracy of the MD program is to test its work for the cases when the exact solution of the problem is known, for example, when the nonlinear interactions are replaced by the linear ones. For conservative systems there is also the standard test consisting in checking the energy conservation. Typically in the MD calculations the total energy must be conserved with an accuracy of  $0.05 \div 1\%$ . (In practice, this test is realized by calculation of the total energy at given time moments, e.g., at each 100-th time step of  $\Delta t$ .) Note that in some schemes of solution of motion equations the energy conservation is supported artificially (e.g., see [72, 73]); in this case we need to look for other methods to test the accuracy.

To finish with the model construction, we have to choose appropriate initial conditions. The choice of the initial configuration depends on the problem under consideration. When we are investigating the system which is close to the exactly integrable one (as, for example, in solitonic problems, see below Chapter 6), it is natural to take one of the exact solutions of the corresponding integrable system (e.g., the state with one or two solitons) as the initial configuration. In investigation of statistical properties of gases or liquids we may take the configuration with random positions of atoms. When we are studying the thermodynamical properties of crystals, it would be better to take the regular arrangement of atoms in the crystal lattice at the initial time moment, but to randomize their velocities. The initial conditions should be chosen with a sufficient attention, because an inappropriate initial state may lead to a metastable configuration which will not be escaped for a reasonable modeling time.

In any case, however, we cannot take the “absolutely correct” initial configuration, because for this we have to know the exact solution of the given problem. Therefore usually we have to wait for some time during which the system will reach the “working” regime, and only after that we may start the calculation of the characteristics under investigation. For example, when we study the equilibrium system parameters, the

“waiting” time corresponds to achieving the equilibrium state. In “solitonic” problems during the waiting time the elementary excitations of the system should take their stationary (“true”) shape. The waiting time depends on the problem under consideration, and it may be about  $(0.25 \div 0.5)t_{\max}$ .

In the next Sections 3.2 to 3.4 we present characteristic examples of the MD modeling, and in the last Sections 3.5 and 3.6 we discuss some important technical details of the application of the MD method.

## 3.2 Melting of two-dimensional crystals

### 3.2.1 Introductory remarks

The checking of validity of the main hypotheses of the statistical mechanics was among the first applications of the MD method. Namely, if we take a real (i.e., anharmonic) potential of interaction between atoms and start from an arbitrary configuration, will the thermal equilibrium state (i.e. the state where the kinetic energy is equally shared among all system degrees of freedom) be achieved with time evolution? The answer which was obtained in the modeling of the one-dimensional atomic chain with the first computer “ANIAC”, suddenly appeared to be negative. This phenomenon, named the Fermi-Pasta-Ulam paradox, will be considered in a more detail below in Sec. 6.1. Note only that the reasons for the negative answer were a small capacity of early computers that did not allow to wait for achieving the equilibrium state, and the using of the one-dimensional model which is characterized by very specific properties.

The two-dimensional model already does not exhibit such a surprise. For example, let us consider the Benettin and Tenenbaum simulation [74], where the two-dimensional system of  $10 \times 10 = 100$  atoms has been investigated. They have used the fixed boundary conditions so that the positions of  $4 \times 9 = 36$  atoms were kept fixed at the boundary of the square box, and  $N = 8 \times 8 = 64$  atoms were allowed to move. The atoms interacted via the LJ potential with the parameters adopted to describe the interaction of argon atoms. The configuration with random coordinates and velocities of atoms was taken as the initial one. Then the Newton motion equations were solved with the time step  $\Delta t = 0.05$  (in the natural for the given problem system of units) during the time  $t_{\max} = 2 \times 10^4$ , and a time  $\sim 10^2$  was given for the system relaxation. The distribution of the energy over the linear modes as well as the auto- and cross-correlation functions and the Fourier spectrum were investigated. The results show (see Fig. 3.4) that the thermal equilibrium state is achieved for a time  $\sim 10$  provided the system energy exceeds the value  $E_{\text{crit}} \approx 0.03N$ , that corresponds to the temperature  $\sim 3\text{K}$  for the chosen model parameters. The existence of the critical energy  $E_{\text{crit}}$  which is nothing else that the threshold of the transition to the developed chaos (see the previous Chapter 2), is caused by a small number of atoms in the system; it has to be expected that  $E_{\text{crit}} \rightarrow 0$  in the limit  $N \rightarrow \infty$  [55].

When the existence of the thermal equilibrium has been proved, we may begin the investigation of properties of the equilibrium state. Recall that for an analytical description of the equilibrium state we usually should have some “small parameter”. For example, in gases the kinetic energy of atoms (molecules) essentially exceeds the potential energy of their interaction, and the latter may be accounted with the help of a perturbation theory. On the other hand, in crystals the atoms take the regular lattice sites and only slightly vibrate with respect to equilibrium positions, so that the kinetic energy plays the role of a small perturbation. But in liquids where the kinetic and potential energies are of the same order, an analytical description becomes very complicated and inexact, and the MD simulation becomes to be practically the only reliable method of the investigation [75].

An another example where the computer modeling plays an important role, is the investigation of phase transitions between different phases. Recall that the phase transition (PT) may be either discontinuous (the first-order PT) or continuous (the second-order PT). From the physical viewpoint the difference between the first-order and second-order PTs consists in the following [76]. In the first-order PT which takes place with changing of some system parameter, e.g., the temperature  $T$ , at a certain value  $T_c$  the free energies of two different phases becomes equal each other. The discontinuous PT is carried out “locally” in space. For example, with  $T$  decreasing at  $T \leq T_c$  nucleus (islands, drops, grains, *etc.*) of the new phase are

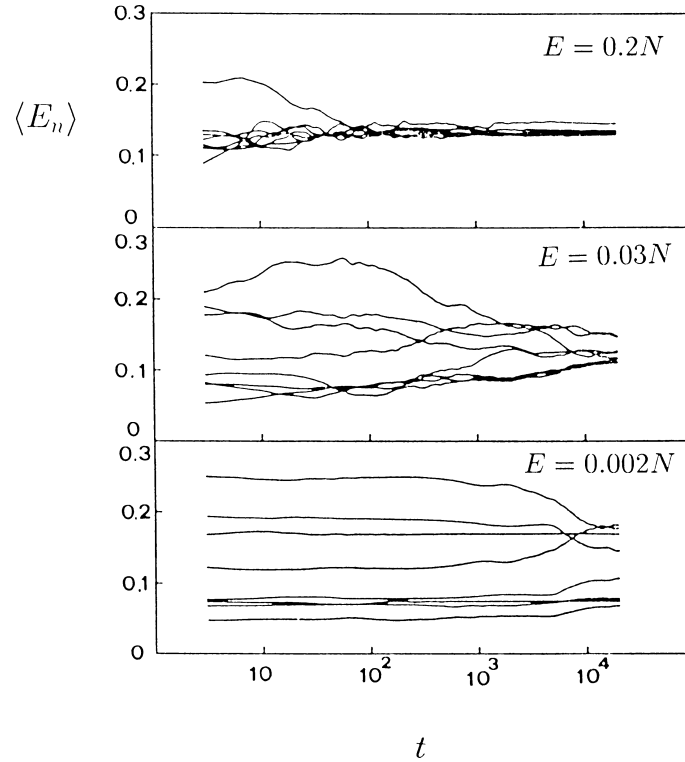


Figure 3.4: Averaged energies  $\langle E_n \rangle$  of the groups of normal modes at three energies, as functions of the averaging time  $t$ .  $E$  is the total energy of the system (after [74]).

spontaneously created at random sites (or at irregularities if those exist) in the system, and when the nucleus reaches some critical size, it will grow up to macroscopic sizes (see below Chapter 5). However, at  $T < T_c$  the old phase may exist as well in a metastable state (for example, the overcooled liquid or gas). Therefore, the main characteristic feature of the discontinuous phase transition that has to be observed in laboratory or computer experiment, is the existence of a hysteresis. Note that for the existence of the first-order PT, there must be an attraction (or at least an “effective” attraction, i.e. the lowering of the interatomic repulsion when the atoms gather together) between the atoms.

The second-order PT is the transition between two phases, one of which must have the lower symmetry than the another phase, i.e. the symmetry group of the first phase should be a subgroup of the symmetry group of the second phase. The continuous PT is carried out by the fluctuation mechanism: when  $T$  decreases approaching to  $T_c$  (but  $T > T_c$ ), “domains” of the new phase are appearing from time to time due to fluctuations, and these domains have a finite (microscopic) lifetime. The closer is  $T$  to  $T_c$ , the larger are the sizes and lifetimes of these domains, and at  $T = T_c$  they occupy the whole space, so that at  $T < T_c$  the old phase exists already as fluctuating domains only. The second-order PT takes place in the whole space simultaneously, and the hysteresis is absent.

The classical example of the phase transition is the melting of the crystalline structure, i.e. the crystal–liquid or order–disorder transition. From experiments we know that this phase transition is the first-order PT usually. However, there are no restrictions which forbid for the melting to be the continuous PT in some systems. An interesting system where the melting is the continuous phase transition, is the two-dimensional Coulomb gas.

### 3.2.2 Physical model

As was first shown by Peierls [77, 78] and Landau [79] (see also [80] and [76]), the existence of the long-range order in a system is connected with the system dimensionality first of all. Let the function  $u(\vec{r})$  describes the displacements of atoms situated near the point  $\vec{r}$ , from their regular positions in the nodes of the ideal crystal lattice. Then as the criterion of the crystalline order, we may consider the behavior of the function

$$\delta^2(\vec{r}) = \langle [u(\vec{r}) - u(0)]^2 \rangle, \quad (3.9)$$

which describes the mean-square displacement of atoms separated by the distance  $\vec{r}$ , with respect to one another. Clearly that in the crystalline phase the limit of the function  $\delta^2(\vec{r})$  must be finite as  $r \equiv |\vec{r}| \rightarrow \infty$ , while in the disordered phase the value  $\delta^2(\vec{r})$  will increase unboundedly. The function  $\delta^2(\vec{r})$  can be estimated if we turn to normal modes,

$$u(\vec{r}) = \int d\vec{q} u_{\vec{q}} \exp(i\vec{q}\vec{r}), \quad (3.10)$$

and then estimate the elastic energy of the system in the harmonic approximation as

$$E \sim \int d\vec{r} \left( \frac{\partial u(\vec{r})}{\partial \vec{r}} \right)^2 \sim \int d\vec{q} q^2 |u_{\vec{q}}|^2. \quad (3.11)$$

Because each degree of freedom has to take an energy  $\sim k_B T$ , the following estimation follows from Eq. (3.11):

$$|u_{\vec{q}}|^2 \sim k_B T / q^2. \quad (3.12)$$

Substituting Eqs. (3.10–3.12) into Eq. (3.9), at  $r \rightarrow \infty$  we approximately obtain (see details in [80]) that

$$\delta^2(r) \sim T \int_{2\pi/r} d\vec{q} q^{-2}, \quad (3.13)$$

where we have to take into account the lower integration limit only.

In the three-dimensional case, where  $d\vec{q} \propto q^2 dq$ , the integral (3.13) is finite, and a crystalline order may exist in the system (of course, when the temperature is low enough). On the other hand, in the one-dimensional system, where  $d\vec{q} = dq$ , the integral (3.13) linearly diverges with  $r$  at  $r \rightarrow \infty$ ,  $\delta^2(r) \propto Tr$ . This means that in one-dimensional systems at any  $T \neq 0$  the disordered phase can exist only, and the PT critical temperature is  $T_c = 0$  (note that the reasons given above assume the short-range interatomic interaction).

In the intermediate case of the two-dimensional system, where  $d\vec{q} \propto q dq$ , the function  $\delta^2(r)$  rises with  $r$  at  $r \rightarrow \infty$  too,  $\delta^2(r) \propto T \ln r$ . But now this growth is logarithmic, i.e., it is not so fast as in the one-dimensional model or in the disordered phase. Thus, although the two-dimensional system cannot exhibit the real crystalline structure, a more or less ordered phase must exist at low temperatures. This phase got the name *floating phase*, or the phase with quasi-long-range order [81].

There is a number of physical systems which may be considered approximately as two-dimensional ones. For example, it may be a film of atoms adsorbed on the crystal surface in the case when we can neglect by the substrate potential relief. As other examples we may mention the system of electrons “levitating” over the surface of liquid helium, or the electrons within the inversion layer in the silicon MOS transistor.

Thus, in the two-dimensional system at a low temperature it should exist the floating phase. On the other hand, at high temperatures the disordered phase has to exist, because it has a higher entropy than the ordered phase. Naturally it arises the question on the temperature and the mechanism of melting of the floating phase. The theory of this phase transition has been proposed by Kosterlitz and Thouless [82]. It is interesting that the two-dimensional melting was first observed in the computer simulation with the help of the MD method (namely, the  $P^3M$  method, see below Sec. 3.5) [83], and only after this, the verification in the laboratory experiment has been followed [84]. Below we briefly discuss the Kosterlitz-Thouless (KT) melting mechanism, and then describe in more detail the MD simulation results of Bedanov *et al.* [85].

According to the KT theory, the two-dimensional system melts by the dislocation mechanism. Namely, a pair of dislocations with opposite signs may be created in the ordered phase. From dislocation theory

it is known (e.g., see [86]) that in the two-dimensional system the two dislocations with opposite signs (i.e., with the opposite directions of Burger's vector) attract each other according to the logarithmic law, so that the creation of the pair increases the system energy on a value  $\sim \varepsilon_0 \ln r$ , where  $\varepsilon_0$  is some energy constant and  $r$  is the distance between the dislocation centers. On the other hand, the dislocation pair can be placed in the lattice in  $\sim (L/a_0)^2$  ways, where  $L$  is the linear system extension and  $a_0$  is the mean interatomic distance. Thus, the creation of the dislocation pair increases the system entropy on a value  $\Delta S \sim k_B \ln(L/a_0)$ . Therefore, the creation of the pair with its consequent dissociation (i.e., the separation of the dislocations for a distance  $r \sim L$ ) changes the free energy of the system on the value

$$\Delta F \sim \varepsilon_0 \ln L - k_B T \ln L. \quad (3.14)$$

From Eq. (3.14) we see that at  $T > T_c \sim \varepsilon_0/k_B$  the creation of free dislocations becomes energetically favorable, so that they have to arise abundantly and, consequently, to destroy the order in the system.

In a more careful consideration of the dislocation melting mechanism we have to take into account that the crystalline phase is to be characterized by two order parameters, namely by the *translational order parameter* and the *orientational order parameter*. The translational order assumes the periodicity in atomic arrangement, which is exhibited, for example, in the existence of clear X-ray diffraction picture. It is described by the correlation function

$$G_r^{(q)}(r) \propto \langle \rho^{(q)}(0) \rho^{(q)}(r) \rangle, \quad (3.15)$$

where  $\rho^{(q)}(r) = \exp[i\vec{q}\vec{u}(r)]$  is the Fourier transform of the density function. The orientational order is connected with the constancy of the crystallographic directions, so that the vectors  $\vec{e}_{kk'}$  which connect the atom  $k$  (occupying the lattice node with the coordinate  $\vec{r}_k$ ) with the neighboring atoms  $k'$ , have a tendency to be parallel or to create fixed angles with analogous vectors in other places of the crystal. The orientational order is described by the correlation function

$$G_\varphi(r) \propto \langle \psi(0) \psi(r) \rangle, \quad (3.16)$$

where

$$\psi(r) = \frac{1}{N} \sum_{k=1}^N \delta(r - |r_k|) \frac{1}{\nu_k} \sum_{k'=1}^{\nu_k} \exp(i\nu\theta_{kk'}), \quad (3.17)$$

$\theta_{kk'}$  is the angle between some fixed axes and the vector  $\vec{e}_{kk'}$ ,  $\nu$  is the number of the nearest neighboring nodes in the lattice (for the triangular lattice  $\nu = 6$ ), and  $\nu_k$  is the number of the nearest neighbors for the given atom  $k$ . In the disordered phase the correlation functions decrease exponentially with  $r$ ,

$$G_r(r) \propto \exp(-r/\xi_r), \quad G_\varphi(r) \propto \exp(-r/\xi_\varphi), \quad r \rightarrow \infty, \quad (3.18)$$

while in the floating phase they decrease according to a power law (recall that in the true crystalline phase the correlation functions oscillate and tend to a nonzero limit at  $r \rightarrow \infty$ ).

At the ordinary melting of the three-dimensional crystal occurring through the first-order phase transition, the both orders disappear simultaneously. But in the floating phase of the two-dimensional crystal, these orders are destroyed by defects of different types: the translational order is destroyed by the creation of dislocation pairs with their consequent dissociation (an isolated dislocation is shown in Fig. 3.5a), while the orientational order is violated owing to the creation and dissociation of disclination pairs (an example of the isolated disclination is presented in Fig. 3.5b). As seen from Fig. 3.5a, the isolated dislocation can be considered as the coupled pair of disclinations with opposite signs. The KT theory predicts that the melting of the floating phase with the increase of temperature may proceed in two stages: first (at  $T = T_{cr}$ ) the translational order is destroyed, and then (at  $T = T_{c\varphi}$ ) the orientational order is destroyed, and both phase transitions are continuous. Thus, within the temperature interval  $T_{cr} < T < T_{c\varphi}$  it should exist a specific phase which has been named the *hexatic* (anisotropic liquid) phase, where the translational order is already destroyed and the correlation function  $G_r(r)$  decays exponentially with  $r$ , while the orientational order still exists so that the function  $G_\varphi(r)$  decays with  $r$  according to the power law.

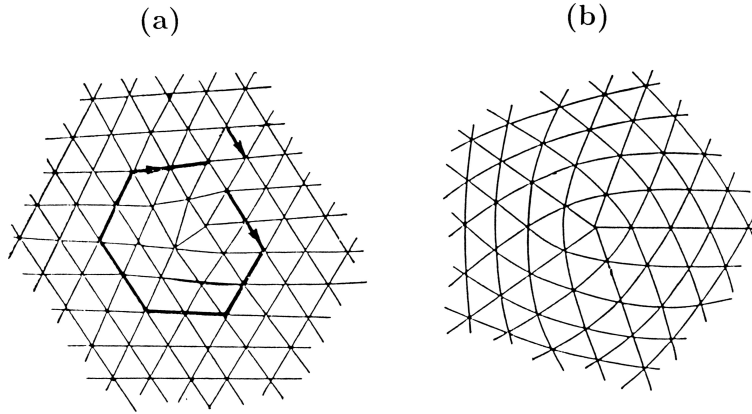


Figure 3.5: Topological defects in a two-dimensional crystal: (a) the isolated dislocation, and (b) the isolated disclination (from [87]).

### 3.2.3 Numerical algorithm

To check the predictions of the KT theory, Bedanov *et al.* [85] considered the two-dimensional system of electrons. The motion equations have the following form:

$$m \frac{d^2 \vec{r}_k}{dt^2} = - \sum_{j (j \neq k)} \frac{\partial V(\vec{r}_j - \vec{r}_k)}{\partial \vec{r}_k}, \quad (3.19)$$

where  $V(\vec{r}) = e^2 / |\vec{r}|$ ,  $m$  is the electron mass, and  $e$  is its charge.

First of all let us demonstrate the choice of units which are natural for the given problem. As the unit of length we take the value  $a_0$  determined by the relationship

$$\pi a_0^2 = 1/n, \quad (3.20)$$

where  $n$  is the two-dimensional concentration of electrons, and as the unit of time we take  $t_0 = a_0/v_0$ , where  $v_0$  is determined by the equation

$$\frac{1}{2} m v_0^2 = \frac{1}{2} k_B T. \quad (3.21)$$

Then it appears that the motion equations involve only a single dimensionless parameter

$$\Gamma = e^2 \sqrt{\pi n} / k_B T. \quad (3.22)$$

In a result, we have to investigate the phase transition with the variation of the single parameter  $\Gamma$ , and then we will be able to describe the phase transition with variation of the temperature  $T$  (for a fixed  $n$ ) as well as the phase transition with variation of the concentration  $n$  (for a fixed  $T$ ).

In the computer experiment it is more convenient to vary the temperature  $T$ . This may be made in the following way: at each step of the solution of the motion equations we rescale the velocities of all atoms,

$$v_i \rightarrow v_i(1 + \varepsilon), \quad (3.23)$$

where  $\varepsilon$  is some small constant ( $\varepsilon > 0$  for increasing of temperature and  $\varepsilon < 0$  for its decreasing) which is to be chosen at “training” of the program. This procedure continues until the necessary value of  $T$  is reached (usually it takes  $\sim 10^2$  time steps). Recall that according the definition, the value  $\frac{1}{2} k_B T$  has to be equal to the average kinetic energy per one degree of freedom of the system.

Because the electrons repel each other, we expect that the floating phase has the structure of the triangular lattice. At the simulation [85] the system was imbedded into the rectangular box, and the periodic

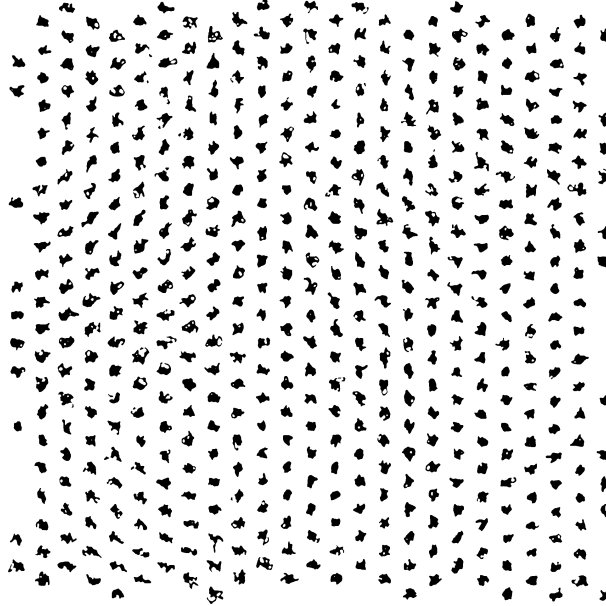


Figure 3.6: Two-dimensional crystal in the floating phase (after Bedanov *et al.* [85]).

boundary conditions were used. In order that the system is to be closed into tori without distortions of the triangular lattice, a certain condition for a possible number of atoms should be satisfied. In the work [85] the authors took  $N = 2(12 \times 21) = 504$ . For the initial configuration the atoms were placed to regular sites of the triangular lattice, while their velocities were set in a random way. Then the system was allowed to relax to equilibrium for a time  $\sim 10^3$  time steps, and during the next  $\sim 10^3$  time steps different system characteristics such as the correlation functions, were calculated. Then the temperature was changed and, after the relaxation to a new equilibrium state, the calculation was repeated.

### 3.2.4 Results of simulation

The simulation results of Bedanov *et al.* [85] are presented in Figs. 3.6 to 3.8. For example, Fig. 3.6 demonstrates a typical arrangement of atoms for the floating phase, and Fig. 3.7, a configuration for the disordered phase. The melting was observed in the interval  $145 < \Gamma < 159$ . This result is in agreement with the experimental results for electrons over the surface of liquid helium, where the melting was observed at  $\Gamma = 137 \pm 15$  [84]. Snapshot pictures directly demonstrate the creation of topological defects and their evolution, i.e., the transformation of coupled dislocation pairs to free dislocations (disclination pairs) and then to free disclinations as the temperature increases. To reveal the hexatic phase, the correlation functions (3.15) and (3.16) were calculated, and then the long-distance tails of the correlation functions were approximated with the help of the mean-square method by simple functions, the exponential functions (3.18) or the power function  $G_{r,\varphi}(r) \propto r^{-\nu}$ . The phase transition should be followed by the change of the asymptotic behavior of the correlation functions so that the exponent  $\nu$  or the correlation length  $\xi$  have to change. Simulation results presented in Fig. 3.8 show that it does exist the temperature interval where the orientational order still exists but the translational order is already destroyed. Thus, the MD modeling validates the KT theory of dislocation melting for the two-dimensional Coulomb system.

In conclusion let us briefly discuss other interesting results of computer simulation of the melting process. First, the two-stage topological melting has been observed for the two-dimensional Coulomb system only. When atoms in the two-dimensional system interact according to the dipole-dipole or LJ law, the MD simulation shows one-stage melting of the floating phase by the first-order phase transition [85]. If the two-dimensional system is subjected to an external periodic potential, phases with usual (long-ranged)

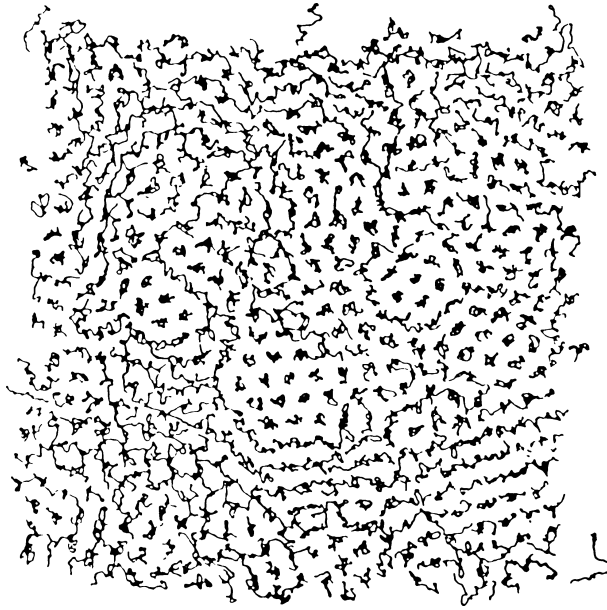


Figure 3.7: Two-dimensional liquid (after Bedanov *et al.* [85]).

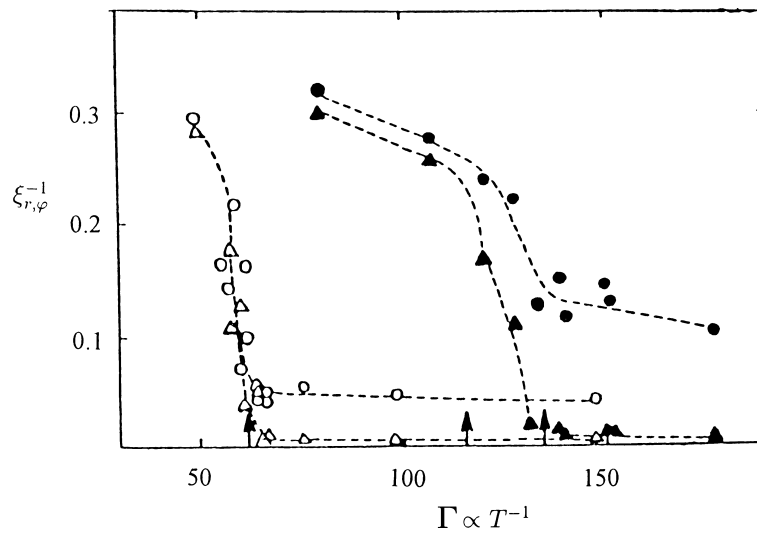


Figure 3.8: Inverse correlation lengths  $\xi_r^{-1}$  (triangles) and  $\xi_\phi^{-1}$  (circles) versus the dimensionless parameter  $\Gamma$  for the Coulomb (full) and dipole (open) two-dimensional systems (after Bedanov *et al.* [85]).

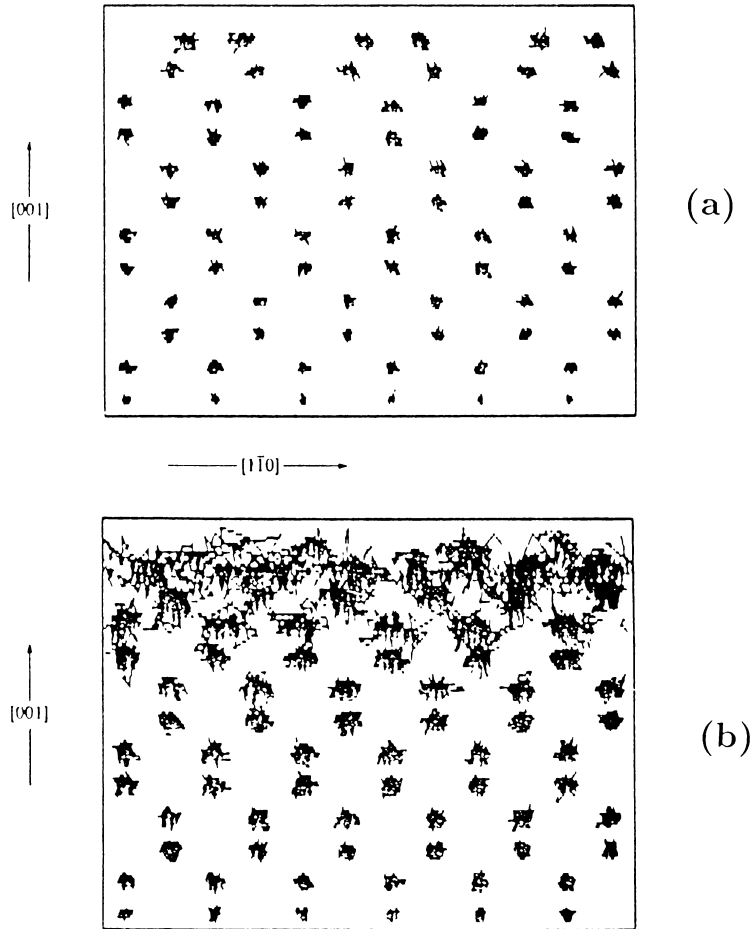


Figure 3.9: Surface melting. Atomic trajectories of the MD simulation for the **Si(100)** surface for (a)  $T = 1003$  K, and (b)  $T = 1683$  K (after Abraham [88]).

crystalline order may exist in the system. When the amplitude of the external potential is high enough (as it is, for example, in films of gas atoms chemically adsorbed on a crystal surface), it is better to use the lattice-gas model which is equivalent to the Ising model with an external magnetic field. The Ising model is to be investigated by the Monte Carlo method described in Chapter 5. Otherwise, when the amplitude of the external potential is small, “solitonic” structures (see Chapter 6) may exist in the system, and the latter may be in the floating phase and to melt by the KT mechanism. A more detailed discussion of these questions can be found, e.g., in the monograph [87].

Finally, melting of a three-dimensional crystal exhibits interesting features too. According to the simplest melting scenario, an amplitude of vibrations of crystal atoms increases as the temperature rises, and when this amplitude achieves some critical value, i.e., when the amplitude becomes so high that the crystalline order is to be destroyed, the crystal melts (the so-called Lindeman criterion). However, a real crystal always has a surface. Because the surface atoms have a lower number of nearest neighbors than the bulk atoms, the amplitude of vibrations for the surface atoms should be larger than that for the bulk atoms. This reason makes the base for the assumption that the surface layers may melt before the bulk ones, i.e., that a thin surface layer has to melt at a temperature  $T'_c$  which is lower than the bulk melting temperature  $T_c$ , and the width of the melted surface layer should increase to infinity as  $T$  approaches to  $T_c$ . The MD simulation [88] indeed directly demonstrates such surface melting (see Fig. 3.9). Laboratory experiments also validate that in some systems the melting process indeed starts from the surface.

### 3.3 Surface diffusion

#### 3.3.1 Introductory remarks

The MD method is of a large value in investigations of kinetic and dynamic characteristics of systems in the thermal equilibrium state. In a general case these characteristics are expressed through different spacial and time correlation functions of the system. Correlation functions contain the complete information on the equilibrium state and, besides, they describe the linear response of the system to an infinitesimal external perturbation.

Many of correlation functions can be directly measured in spectroscopy experiments. All spectroscopy methods are based on the irradiation of the sample with some particles (photons, electrons, positrons, neutrons, ions, atoms, molecules) and the measuring the energy and angular distribution of scattered particles. Different spectroscopy methods help to get a rich information on the system under investigation. For example, the positions of peaks (more rigorously, hollows) in the energy distribution give the frequencies (energies) of elementary excitations (quasiparticles) in the system, while the width of the corresponding peak as well as its shape contains the information on the quasiparticle dynamics. However, an extraction of this information is often a rather difficult problem, and typically it is done with the help of comparison of experimental spectra with those predicted theoretically (e.g., see review papers [89] and [90]). For example, the line width in the vibrational spectrum is caused by damping of a given mode, i.e. by the rate  $\eta$  of the energy exchange between the mode and other elementary excitations of the system. The measuring of  $\eta$  is very important because the value of  $\eta$  determines in an essential degree the system dynamics. But additionally to  $\eta$ , two more mechanisms lead to contributions into the line width. There are the so-called *inhomogeneous broadening*  $\eta_x$  and *dephasing broadening*  $\eta_t$ . The first contribution  $\eta_x$  is coupled with a spacial disorder in the system, i.e., with the existence of defects of the crystalline structure, impurities, *etc.* The dephasing broadening  $\eta_t$  is caused by a temporal chaos of the system, i.e. by its nonintegrability. Note that in some systems the ratio  $\eta_t/\eta$  may achieve so large values as  $10^2$ . The extraction of different contributions into the line width, is in need of the corresponding theory. In developing of this theory the MD simulation plays a significant role. As examples we can mention the works [69] and [91].

Different transport coefficients such as the diffusion coefficients are important characteristics of the system too. The diffusion plays a large role in many processes which are important from the practical viewpoint, for example, in crystal growth or in heterogeneous catalytic reactions, and also in microelectronics, *etc.* [92, 93]. There are three different diffusion coefficients: the self-diffusion coefficient, the collective diffusion coefficient (coupled with the system conductivity by Einstein's relationship), and the chemical diffusion coefficient (the latter appears in the first Fick law). All diffusion coefficients are defined through the velocity correlation functions. In particular, the self-diffusion coefficient is defined as

$$D_s = \frac{1}{\nu} \frac{1}{N} \sum_{i=1}^N \int_0^\infty dt \langle \vec{v}_i(0) \vec{v}_i(t) \rangle, \quad (3.24)$$

where  $\nu$  is the system dimensionality ( $\nu = 2$  for the surface diffusion).  $D_s$  describes the Brownian motion of a given particle,

$$\langle [\vec{r}_i(t) - \vec{r}_i(0)]^2 \rangle \simeq 2\nu D_s t \text{ at } t \rightarrow \infty. \quad (3.25)$$

Below we consider one concrete example of investigation of the self-diffusion by the MD method.

#### 3.3.2 Diffusion of Na atom adsorbed on the surface of Na crystal

De Lorenzi and Jacucci [94] have investigated by the MD method the self-diffusion of the **Na** atom adsorbed on the surface of the **Na** metal crystal. The b.c.c. **Na** crystal was modeled as a parallelepiped of  $N$  atoms. The number  $N$  depends on the surface under investigation. De Lorenzi and Jacucci [94] have modeled three crystallographic faces: the (112) face which has a furrowed (channelled) structure, was modeled by a slab of  $N = 288$  atoms (12 planes,  $3 \times 8$  atoms in each plane), the densely packed (compact) (110) face was modeled

by  $N = 240$  atoms (8 planes, 30 atoms in each plane), and for the comparatively rare (loosely packed) (100) face it was taken  $N = 250$  atoms (10 planes, 25 atoms in each plane). The periodic boundary conditions were imposed on the side planes of the parallelepiped, while the top surface and the bottom surface were left free (the “working” surfaces).

In order to model the crystal with the b.c.c. lattice, the authors had to use the realistic potential for the interaction between the **Na** atoms, because with the 12-6 LJ potential the sample relaxed to the f.c.c. lattice. The potential  $v(r)$  was calculated preliminary with the help of the pseudopotential technique, and then it was tabulated with the step  $0.00123 a_0$  ( $a_0 = 4.30 \text{ \AA}$  is the lattice constant of the **Na** crystal). The real potential  $v(r)$  differs from the LJ potential by that the former is nonmonotonic — it has a small maximum at the distance  $r \sim 2a_0$  (the so-called Friedel oscillations).

The question on the initial conditions was solved in an original way. Namely, one atom was taken off from the bottom surface and placed on the top surface of the parallelepiped. Due to this trick two problems were solved simultaneously in a single simulation run, namely the problem of diffusion of the extra atom (adatom) on the top surface, and the problem of diffusion of the vacancy in the bottom surface.

The choice of the temperature  $T$  in computer simulation of such a type is determined by two factors. On the one hand, at low  $T$  the adatom will move too slowly, and for a realistic simulation time we will not achieve the asymptotic (3.25) and, therefore, will not have the necessary number of simulation runs in order to find a reliable value of  $D_s$ . On the other hand, at high  $T$  the probability of fluctuationally-driven generation of new adatom–vacancy pairs is high, and at  $T \geq T'_c$  the surface will be melted at all. According to the work [94], the choice  $T = 0.4T_c$  is the optimal one.

During the simulation the initial time interval was given for relaxation to the equilibrium state. During this initial time period the Newton motion equations were replaced by the Langevin equations (see the next Chapter 4) in order to accelerate the relaxation and to avoid the situation when the system catches itself in a metastable state. At the same time during the initial time interval the temperature was slowly increased from zero to the given value  $T = 0.4T_c$ .

The trajectories of the adatom motion obtained in the MD simulation, are presented in Figs. 3.10 to 3.12. On the furrowed (112) face (see Fig. 3.10) the diffusion is strongly anisotropic, the adatom moves along the channels only. Sometimes, however, the so-called “exchange” diffusion takes place, when the adatom  $A$  “push out” the surface atom  $B$  from its regular position in the row of surface atoms, and occupies the created free site. In the new configuration we again have the single adatom ( $B$ ) which, however, is now in the nearest neighboring furrow. Thus, in this way an effective diffusion across the furrows takes place. The diffusion across the furrows is about ten times slower than the diffusion along the furrows. Comparison of the results for the (110) and (100) faces (see Figs. 3.11 and 3.12 respectively) shows that on a more “crumbly” (100) face the adatom moves essentially slower than on the smooth (110) face. The qualitative picture of surface diffusion obtained in the simulation, is in agreement with the experimental results obtained for the diffusion of atoms adsorbed on the metal surfaces with the help of the field ion microscopy (e.g., see [92]).

Note that the computer simulation [94] demonstrates also “long jumps” (i.e., the jumps of the adatom for distances of a several lattice constants at once without stops in the intermediate adsorption sites) which, however, were not observed in laboratory experiments. The existence of the long jumps in the simulation is probably caused by the too low value of the effective damping in the model used by the authors [94]. Indeed, they took into account a single friction mechanism (i.e., the mechanism of energy exchange between the moving adatom and the substrate) only, namely, the phonon friction which corresponds to the adatom energy losses owing to creation of vibrations of substrate atoms. But in the case of the metal substrate the “electron-hole” friction mechanism, i.e., the energy losses due to creation of electron-hole pairs in the substrate, plays an essential role as well [90]. With accounting of this additional friction, the long jumps have to become improbable.

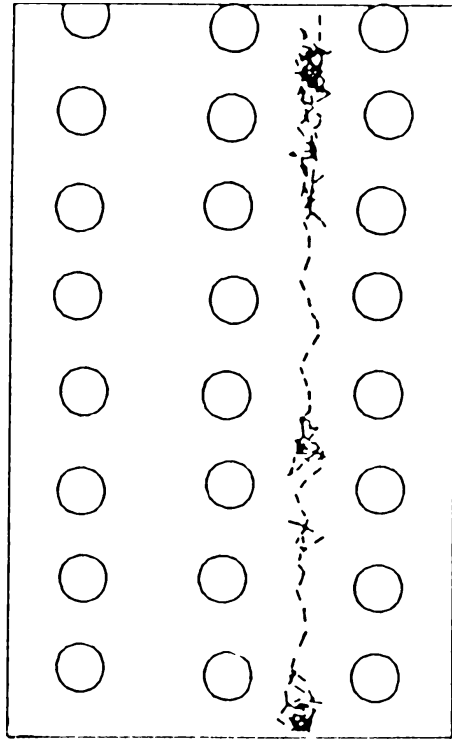


Figure 3.10: Adatom strolling along a channel on the b.c.c. (112) surface, in a 1000 time steps ( $\sim 20$  ps) run as calculated by De Lorenzi and Jacucci [94].

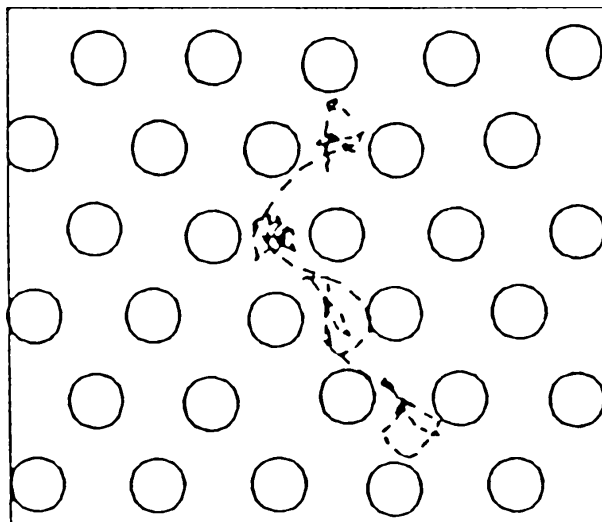


Figure 3.11: Adatom migration on the b.c.c. (110) surface. The positions of the surface atoms at the beginning of the interval are shown as open circles (from [94]).

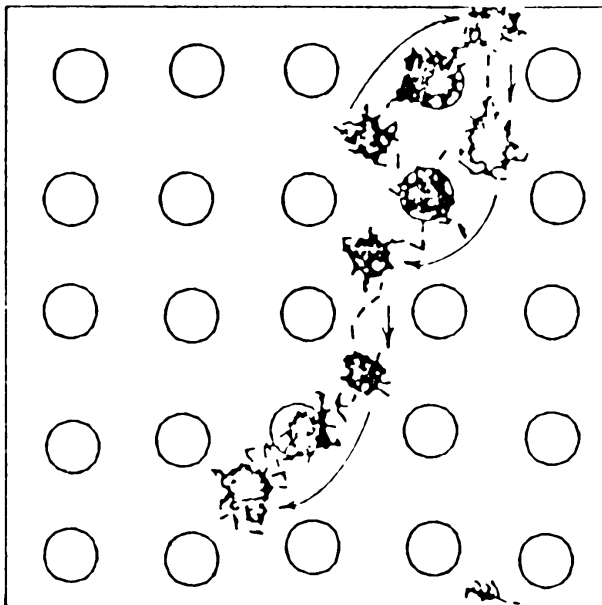


Figure 3.12: Adatom migration on the b.c.c. (100) surface, during a run of 100 ps. The positions of all the surface atoms at the beginning of the run are represented with circles; only the trajectories of the adatom originally present on the surface and of the surface atoms directly interested by its migration are represented. Short straight arrows indicate direct jumps of the adatom from one equilibrium site on the surface to another. Longer curved arrows indicate exchange events, in which the adatom changes identity (from [94]).

### 3.4 Epitaxial crystal growth

One more class of systems where the MD simulation plays a large role, is the class of systems far from the thermal equilibrium state. First, the MD simulation helps to consider the process of relaxation to equilibrium. Second, we can investigate the systems which are in a steady state, i.e., in the stationary but nonequilibrium state. Nonequilibrium state may be supported by a flux of energy or particles from outside. As an example, in the present section we consider the second from the mentioned processes, namely the epitaxial crystal growth. In this process certain atoms are placed into the defined sites of the substrate, so that in the result we obtain, e.g., a chip with given characteristics. But in order to control this process and to grow the crystal with the given parameters, we have to answer to the following questions: **(a)** What should be the velocity of arriving atoms? **(b)** At what angle should we direct the incoming beam? **(c)** What should be the substrate temperature?

Indeed, if the energy of the arriving atom and the substrate temperature are small, the atom which comes to the surface at a random site, will be “pinned” at this site because the atom will have no enough energy to migrate along the surface. In the result, the obtained structure will be disordered, and the growing crystal will be amorphous. On the other hand, the increase of the energy of the incoming beam will lead either to creation of defects in the substrate or to sputtering of the latter. Thus, in order to grow a more or less perfect crystal, we have to find an optimal regime at which the atom which comes to the surface, will migrate along the surface for some time looking for a “suitable” site with the lowest potential energy.

Note that the incoming atomic beam can be created by two methods. First, we can evaporate a drop of the given substance. In this way we get the atomic beam with thermal velocities. Second, we can sputter the source bombarding it by high-energy ions. In this case we obtain the atomic beam with high velocities. Thus, it arises the question, which method to choose. To answer it, Müller [95] has investigated with the help of the MD simulation the influence of the energy of the incoming atomic beam on the growth of thin films. He

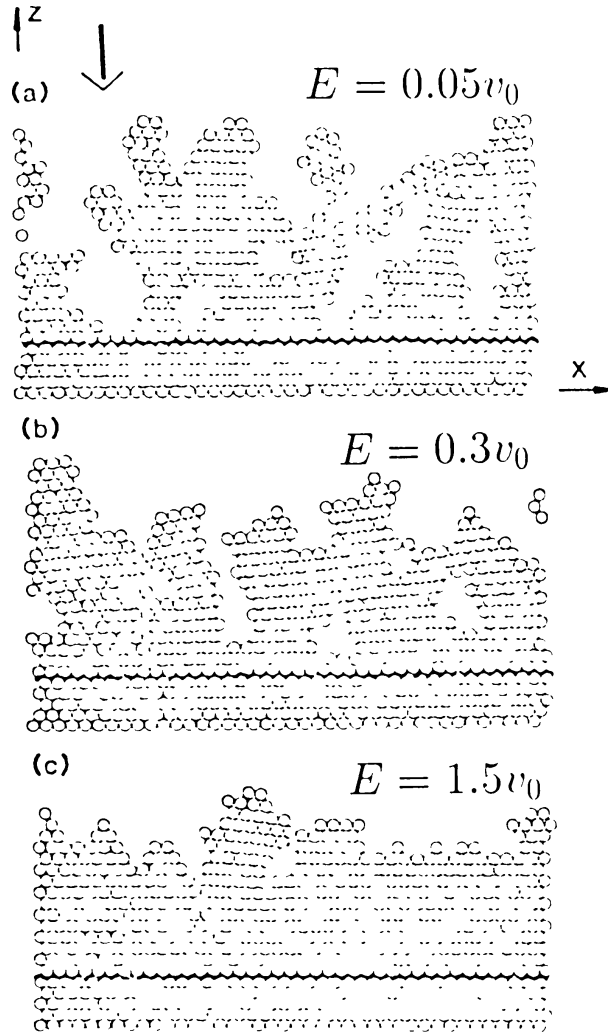


Figure 3.13: Microstructure of the film after deposition of 550 atoms as calculated by Müller [95] for different energies of arriving atoms: (a)  $E = 0.05v_0$ , (b)  $E = 0.3v_0$ , and (c)  $E = 1.5v_0$  ( $v_0$  is the parameter of the LJ potential).

considered a two-dimensional system with a “glass” shape, i.e., the system was restricted by the inequalities  $0 < x < L$  and  $0 < y < \infty$ , where  $L$  is the “glass” width. It was taken  $L = 40a_0$  so that along the  $x$  axis one may place up to 40 atoms in one row. On the side walls of the “glass” the periodic boundary conditions were imposed. For the interaction potential between the atoms it was taken the Lennard-Jones potential (3.5). As the initial configuration it was taken the perfect crystal consisting of five atomic layers placed on the “glass” bottom. The first (lowest) atomic layer was kept immobile (the fixed boundary conditions). As for the atoms from the second layer, it was assumed that, besides the forces from the neighboring atoms, the viscous friction force acts additionally on these atoms. In this way an energy has been taken away from the system. The motion of other atoms was subjected to the Newton motion equations.

On the substrate constructed in this way, from the “glass” top the atoms with a given velocity (energy) directed normal to the crystal surface, and a random  $x$  coordinate were injected one by one. The crystals growing in the simulation, are shown in Fig. 3.13 for different incident kinetic energies of the incoming beam. As seen, at small energy of the arriving atoms (Fig. 3.13a) the microstructure of the growing crystal is “crumbly”, while at high energies the obtaining structure is more or less closely packed (Figs. 3.13b and 3.13c). In the next Fig. 3.14 the average density of the growing crystal versus the incident kinetic energy

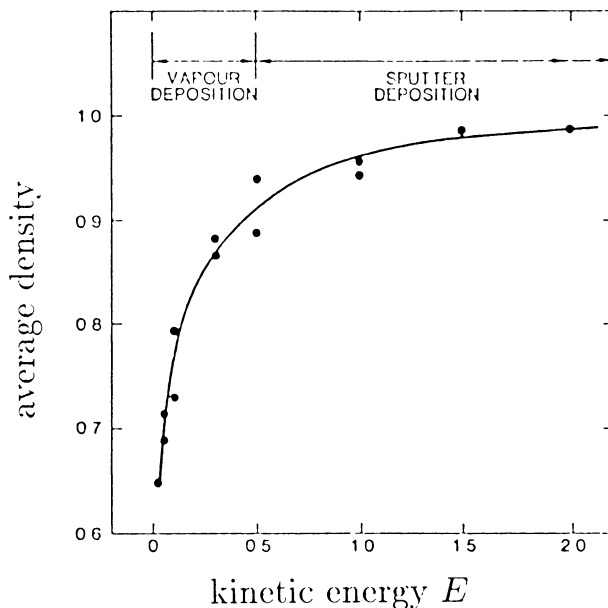


Figure 3.14: Mean density of the growing film versus the kinetic energy of incident atoms (after [95]).

of the incoming atomic beam is presented. As seen, the growth of “good” crystals is achieved only when one uses the beam with high atomic velocities, so the beam from the sputtering sources is to be preferable. Besides, it was found the average distance which the adsorbed atom should “run” in order to get a “true” position in the crystalline lattice — it occurs to be about  $2a_0$ .

### 3.5 PP, PM and P<sup>3</sup>M methods

The “core” of the MD method is the solution of the Newton motion equations for as many particles as possible. It is clear, however, that with the increase of the number of particles  $N$  the computation time raises catastrophically. In the present section we briefly describe special methods which help to reduce the computer time.

In a general case, each particle interacts with all other particles in the system. Therefore for the “direct” accounting of all interactions the computation time will be proportional to  $N(N - 1) \approx N^2$ . Moreover, when we use the periodic boundary conditions, the situation becomes completely catastrophic: although the number of motion equations is  $N$  only, each particle interacts with not only the  $N - 1$  other particles, but with their “images” (see Fig. 3.15) including its own “image”, i.e., with an infinite number of particles! An elegant procedure to sum the forces acting on the given particle from the infinite number of neighboring particles, was proposed by Ewald [96] (see also [97] and, e.g., [98]). Practically, however, the “direct” accounting of all interactions is not used.

The situation simplifies when the interaction potential is short-ranged as, for example, for the 12-6 LJ potential (3.5) or the Morse potential (3.7). In this case we can neglect by interactions of particles separated by large enough distances. To do this, it is introduced the so-called “truncating radius”  $r^*$ , and it is taken into account the interaction of the given particle with those  $N^*$  particles only which occur within the circumference (or the sphere in the three-dimensional case) of the radius  $r^*$  with the center on the given particle. A value of  $r^*$  is typically of the order of  $(2 \div 3)a_0$ , where  $a_0$  is the mean interparticle distance. Note that during the training of the program we should check either the increasing of  $r^*$  changes essentially the simulation results (in particular, this is very important in investigation of first-order phase transitions, see [99]). Owing to fluctuations of the local density of particles, the number of particles which are within the sphere of the fixed radius  $r^*$ , may vary (fluctuate) in time. That leads to some distortion of the computation

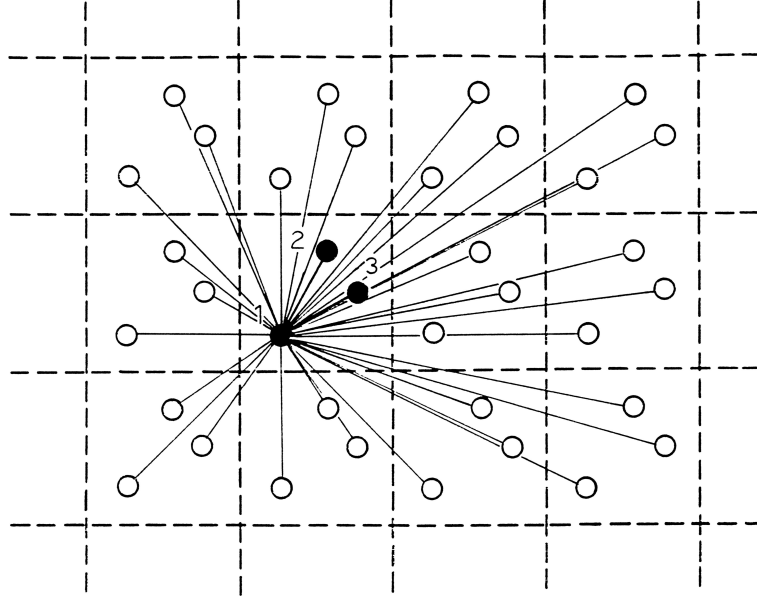


Figure 3.15: Atomic images emerged because of the periodic boundary conditions.

results, because the potential energy changes jump-like with  $N^*$  variation. In practical realization of this method, a special “coupled lists” program is used, where the numbers of the neighboring particles for the each given particle are stored [100]. The method described above, is known as the **PP** (particle-particle) method. Clearly that the computation time in the **PP** method is proportional to  $NN^*$ .

In the case of long-range (Coulomb) interparticle interactions the using of the **PP** method becomes unrealistic even for one-dimensional systems. In this case, however, we can use the **PM** (particle-mesh) method. The idea of the method consists in the following. Let us split the whole system into small cells (squares or cubes) with a side  $r_m$  and take  $r_m \gg r_0$ , so that each cell will contain several particles. Let us consider the forces acting on the given particle from the particles belonging to some sufficiently removed cell. Because these forces are approximately of the same value, their sum can be approximately substituted by a force acting on the given particle from some effective particle placed into the center of the removed cell. Practically this procedure reduces to calculation of the electrostatic potential  $\varphi(r, t)$  (or the gravitation potential in astronomical problems) with the help of the solution of Poisson’s equation  $\Delta\varphi(r, t) = 4\pi\rho(r, t)$  over the mesh with the cell size  $r_m$ , and then to determination of the force acting on the  $k$ -th particle with the charge  $e$  as

$$\vec{F}_k(t) = -e\vec{\nabla}\varphi(r, t) |_{r=r_k}. \quad (3.26)$$

The algorithm of the solution is the following:

- (a) The number of particles in each cell and, consequently, the cell charges  $\rho_i(t)$  are calculated (the so-called procedure of “distribution of charge between the mesh cells”).
- (b) The discrete Poisson equation is solved. For example, in the one-dimensional case this equation has the following form:

$$\varphi_{i-1}(t) - 2\varphi_i(t) + \varphi_{i+1}(t) = 4\pi\rho_i(t). \quad (3.27)$$

Different methods of solution of such equations are described, in particular, in the book [7].

- (c) Using an interpolation procedure, the potential  $\varphi(r, t)$  is found for the points where the particles are situated, and then the forces (3.26) are calculated.
- (d) The motion equations are solved by the Runge-Kutta method.

The **PM** method is used mainly for solution of the plasma physics problems. The computation time in the **PM** method is proportional to  $N_M^\nu$ , where  $N_M = L/r_m$ , and  $\nu$  is the dimensionality of the system ( $\nu=1,2$

or 3). The deficiency of the **PM** method consists in large errors for the forces acting between short-ranged particles.

The quality features of both methods are accumulated in the hybrid **P<sup>3</sup>M** method (**P<sup>3</sup>M=PP+PM**). In this method the force  $F_k(t)$  acting on the particle, is split into two contributions,

$$F_k(t) = F_k^{(\text{short})}(t) + F_k^{(\text{long})}(t), \quad (3.28)$$

where  $F_k^{(\text{short})}(t)$  is the “short-range” contribution caused by interactions of closely situated particles, while  $F_k^{(\text{long})}(t)$  is the “long-range” force acting from the more removed particles. Then the force  $F_k^{(\text{short})}(t)$  is calculated exactly by the **PP** method, while the force  $F_k^{(\text{long})}(t)$  is found with the help of the **PM** method. Comparing with the direct use of the **PP** method, the computation time in the **P<sup>3</sup>M** method is shorter in several orders of magnitude. However, the corresponding computer programs are too complicated [7].

### 3.6 Canonical ensemble

To conclude this Chapter devoted to the MD method, let us discuss in more detail the adaptation of the method to statistical physics problems. First, let us recall that in the MD method the time average (but not the average over ensembles) is calculated, so that the existence of a developed chaos in the system is the necessary condition which must be fulfilled. Second, note that in the standard variant of the MD method we keep fixed the number of atoms, the total system energy and its volume, i.e., we are considering the *microcanonical ensemble*. In thermodynamics, however, the *canonical ensemble* is more often used, when the temperature (the average kinetic energy of atoms) is fixed instead of the energy.

The simplest way (see [101]) of extension of the MD method to the canonical ensemble is to rescale the velocities  $v_l$  at each time step in such a way that the condition

$$\sum_{l=1}^N \frac{1}{2} m_l v_l^2 = \frac{1}{2} \nu N k_B T \quad (3.29)$$

is fulfilled. However, the phase trajectories calculated in this way are discontinuous.

Another method of introduction of the canonical ensemble (see [102, 103, 104]) is to impose the so-called *nonholonomic constraints*, i.e., to add to the system of Newtonian equations the additional condition

$$\sum_{l=1}^N \frac{1}{2} m_l v_l^2 = \frac{1}{2} (\nu N - 1) k_B T. \quad (3.30)$$

The imposing of the constraints leads to appearing of an additional term in the motion equations of the Hamiltonian system, so that the resulting set of equations takes the form

$$\begin{cases} dq_l/dt = p_l/m_l, \\ dp_l/dt = -\partial V/\partial q_l - \alpha p_l, \end{cases} \quad (3.31)$$

where

$$\alpha(t) = -\frac{\sum_l (\partial V/\partial q_l)(p_l/m_l)}{\sum_l p_l^2/m_l}. \quad (3.32)$$

The method described above has the deficiency that the temperature in this method is strictly fixed. Therefore, all fluctuations of the temperature are artificially suppressed, while in the canonical ensemble the temperature always fluctuates, and  $\delta T \propto 1/\sqrt{N}$ . In a result, the calculated distribution function has an error proportional to  $N^{-1/2}$ .

For calculation of the canonical ensemble by the MD method it may be used also the Nosé method [105], which assumes the introduction of an additional degree of freedom  $s(t)$ ,  $p_s(t)$  in such a way that the

distribution function, projected onto the physical system from the extended system of  $N$  particles plus the variable  $s$ , is to be depended exponentially on the system energy (as it just must be for the canonical ensemble). The additional variables  $s(t)$  and  $p_s(t)$  are called usually as “demons”. These “demons” should act in such a way that to keep fixed the system temperature. Namely, let us introduce new variables  $\tilde{q}$ ,  $\tilde{p}$ ,  $\tilde{s}$ ,  $\tilde{p}_s$ , and  $\tilde{t}$  (called the “virtual variables”) related with the real variables by the equations

$$\begin{cases} q_l &= \tilde{q}_l, \\ s &= \tilde{s}, \\ p_l &= \tilde{p}_l/\tilde{s}, \\ p_s &= \tilde{p}_s/\tilde{s}, \\ t &= \int^{\tilde{t}} d\tilde{t}/\tilde{s}. \end{cases} \quad (3.33)$$

Let us postulate the system Hamiltonian for the extended system in the virtual variables in the form

$$\tilde{H}(\tilde{q}, \tilde{p}, \tilde{s}, \tilde{p}_s) = \sum_{l=1}^N \frac{\tilde{p}_l^2}{2m_l \tilde{s}^2} + V(\tilde{q}) + \frac{\tilde{p}_s^2}{2Q} + gk_B T \ln \tilde{s}, \quad (3.34)$$

where the term  $\tilde{p}_s^2/2Q$  corresponds to the “demon” kinetic energy,  $gk_B T \ln \tilde{s}$  describes its potential energy,  $Q$  is the “demon” mass, and  $g$  is the integer constant chosen below.

Hamiltonian (3.34) leads to the following motion equations:

$$\begin{cases} d\tilde{q}_l/d\tilde{t} &= \partial\tilde{H}/\partial\tilde{p}_l &= \tilde{p}_l/m_l \tilde{s}^2, \\ d\tilde{p}_l/d\tilde{t} &= -\partial\tilde{H}/\partial\tilde{q}_l &= -\partial V/\partial\tilde{q}_l, \\ d\tilde{s}/d\tilde{t} &= \partial\tilde{H}/\partial\tilde{p}_s &= \tilde{p}_s/Q, \\ d\tilde{p}_s/d\tilde{t} &= -\partial\tilde{H}/\partial\tilde{s} &= (\sum_l \tilde{p}_l^2/m_l \tilde{s}^2 - gk_B T)/\tilde{s}. \end{cases} \quad (3.35)$$

Then the average over the microcanonical ensemble for the extended system with the “demons”,

$$\langle A \rangle_{\tilde{t}} \propto \int d\tilde{\Gamma}_{\nu N+1} A(q, p, s, p_s) \delta(E - \tilde{H}), \quad (3.36)$$

calculated by the standard MD method for the set of equations (3.35), with accounting of the relationship

$$d\tilde{\Gamma}_{\nu N+1} = d\Gamma_{\nu N} ds dp_s, \quad (3.37)$$

for the case of  $g = \nu N + 1$  may be rewritten in the form

$$\langle A \rangle_{\tilde{t}} \propto \int d\Gamma_{\nu N} A(p, q) e^{-H/k_B T}, \quad (3.38)$$

so that it just coincides with the average over the canonical ensemble for the original model.

Numerical integration of the system of equations (3.35) is too complicated, because the virtual time  $\tilde{t}$  is nonlinearly coupled with the real time  $t$ . Therefore it is more convenient to return to the real variables, that leads to the following system of equations [105]:

$$\begin{cases} dq_l/dt &= p_l/m_l, \\ dp_l/dt &= -\partial V/\partial q_l - sp_s p_l/Q, \\ ds/dt &= s^2 p_s/Q, \\ dp_s/dt &= (\sum_l p_s^2/m_l - gk_B T)/s - sp_s^2/Q, \end{cases} \quad (3.39)$$

which should be solved with the help of a computer. Note that in the latter case the average  $\langle A \rangle$  is to be calculated with the relation

$$\langle A \rangle = \frac{\langle s^{-1} A(p, q) \rangle_t}{\langle s^{-1} \rangle_t}, \quad (3.40)$$

and that we have to set  $g = 3N$  here. As for the “demon” mass  $Q$ , in its choosing we have to come of the facts that at  $Q \rightarrow 0$  the “demon” separates from the system, while at  $Q \rightarrow \infty$  its motion becomes too slow. Therefore we have to take an optimal value for  $Q$  such that the frequency of the  $s(t)$  variation be of the same order as a characteristic system frequency.

Unfortunately, the Nosé method is imperfect too, because it has some additional conserved quantities (for example, the conservation of the total momentum) which disturb the distribution function. Therefore, for the correct simulation of the canonical ensemble we have to use the MD method based on the solution of Langevin equations.

Besides the  $NVE$  (microcanonical) and  $NVT$  (canonical) ensembles, there exist modifications of the MD method which allow to study the  $NPE$  ensemble or the  $NPT$  ensemble as well, where the system volume may change, while the pressure is kept constant (see [105, 1]).